genesis 34:146–151 (2002)

Real-Time Imaging of Morphogenetic Movements in *Drosophila* Using Gal4-UAS-Driven Expression of GFP Fused to the Actin-Binding Domain of Moesin

Devkanya Dutta,[1] James W. Bloor,[2,3] Mar Ruiz-Gomez,[4] K. VijayRaghavan,[1] and Daniel P. Kiehart[2]*

[1]National Centre For Biological Sciences, UAS Campus, Bangalore, India
[2]Developmental, Cell and Molecular Biology Group, Department of Biology, Duke University, Durham, North Carolina, USA
[3]Research School of Biosciences, University of Kent, Canterbury, UK
[4]Centro de Biologia Molecular "Severo Ochoa," UAM-CSIC, Madrid, Spain

Received 3 June 2002; Accepted 9 June 2002

During metazoan development the ongoing process of cell-fate specification channels cells to distinct fates. Once committed, cellular ensembles exhibit tightly coordinated sequences of morphogenetic activities that collectively contribute towards forming the final structure of the organism. These activities involve a wide variety of cell behaviors: individual cells may change shape, divide, or migrate to different areas, entire tissue layers can spread across a surface or fold up to form a three-dimensional structure. A better understanding of such cellular behaviors can be obtained by simply watching them as they occur in a living, unperturbed organism. This forms the basis of the real-time imaging study that is fast becoming a powerful technique for comprehending cellular dynamics.

The advent of green fluorescent protein (GFP) and its engineered and mutagenized variants as viable cellular markers has greatly facilitated non–invasive imaging in different biological systems (Chalfie and Kain, 1998; Tsien and Prasher, 1998). In *Drosophila*, GFP expressed by fusing it downstream of promoter elements has been used to study tissue morphology (e.g., Hazelrigg, 1998; van Roessel and Brand, 2002). However, GFP driven by a ubiquitously expressed promoter/enhancer is not useful for imaging tissues buried deep within the organism and use of a tissue-specific promoter/enhancer restricts study to a particular tissue type. The Gal4-UAS system circumvents these problems and enables fluorescence labeling of desired tissue types by crossing UAS-GFP to appropriate Gal4 drivers (Brand and Perrimon, 1993; Brand *et al*., 1994). Despite this, when expressed alone GFP diffuses within the cell cytoplasm and fails to outline cell boundaries, making its use as a reporter of cell shape changes in live images marginal.

Here we describe the use of UAS-GMA, a chimeric construct that fuses the actin binding region of *Drosophila* moesin to the C-terminus of GFP (Bloor and Kiehart, 2001; and see below). This UAS-GMA construct serves as an excellent marker for tracking live cell morphology because it binds tightly to the cortical F-actin that comprises the majority of cellular F-actin in most cells (see below). Moreover, in our hands this marker outperforms GFP fused directly to actin (Verkhusha *et al.,* 1999), apparently because the signal-to-noise ratio is better: less GMA remains free in the cytoplasm compared to globular, GFP-actin. This empirical observation is supported by what is known about the biochemistry of actin assembly and the interaction of moesin with F-actin. The K_d of actin-binding of vertebrate moesin for F-actin is in the nM range (Nakamura *et al*., 1999), whereas cellular pools of polymerized F-actin (and, therefore, we assume GFP-actin) constitute from 25–60% of the total actin, depending on metazoan cell type (Pollard *et al*., 2000). Because we expect actin to be in significant molar excess over expressed GMA, significantly less than 0.01% of the GMA should be free in the cytoplasm, not bound to F-actin. In contrast, 40–75% of the GFP-actin will be free in the cytoplasm, depending on cell type. In muscle cells, where actin is present in very high concentrations throughout the cytoplasm (sarcoplasm), it also serves as an excellent marker for cell shape.

Moesin is the *Drosophila* homolog of the moesin, ezrin and radixin (MER) group of vertebrate proteins that function as membrane–cytoskeleton linkers (Furthmayr *et al*., 1992). The conserved N terminal "head" domain of the MER family attaches to the membrane proteins, while the C terminal tail binds to F-actin. The DNA sequence that encodes the C terminal 140 amino acids of *Drosophila* moesin and includes the entire actin-binding domain (Edwards *et al*., 1994; see accession NM 080343 for the complete sequence of *Drosophila* moesin) was fused to the human codon bias S65T version of GFP protein to generate the chimeric GMA construct (accession U50963, CLONTECH Laboratories, Palo Alto, CA). The S65T mutation speeds protein folding and in-

* Correspondence to: Daniel P. Kiehart, Developmental, Cell and Molecular Biology Group, Department of Biology, Duke University, B330 LSRC Building, Research Drive, Durham, NC 27708-1000.
All authors contributed equally to this work.
E-mail: dkiehart@duke.edu
Contract grant sponsors: Department of Biotechnology (to KVR), the NIH, the March of Dimes, and the AFOSR (to DPK).

DOI: 10.1002/gene.10113

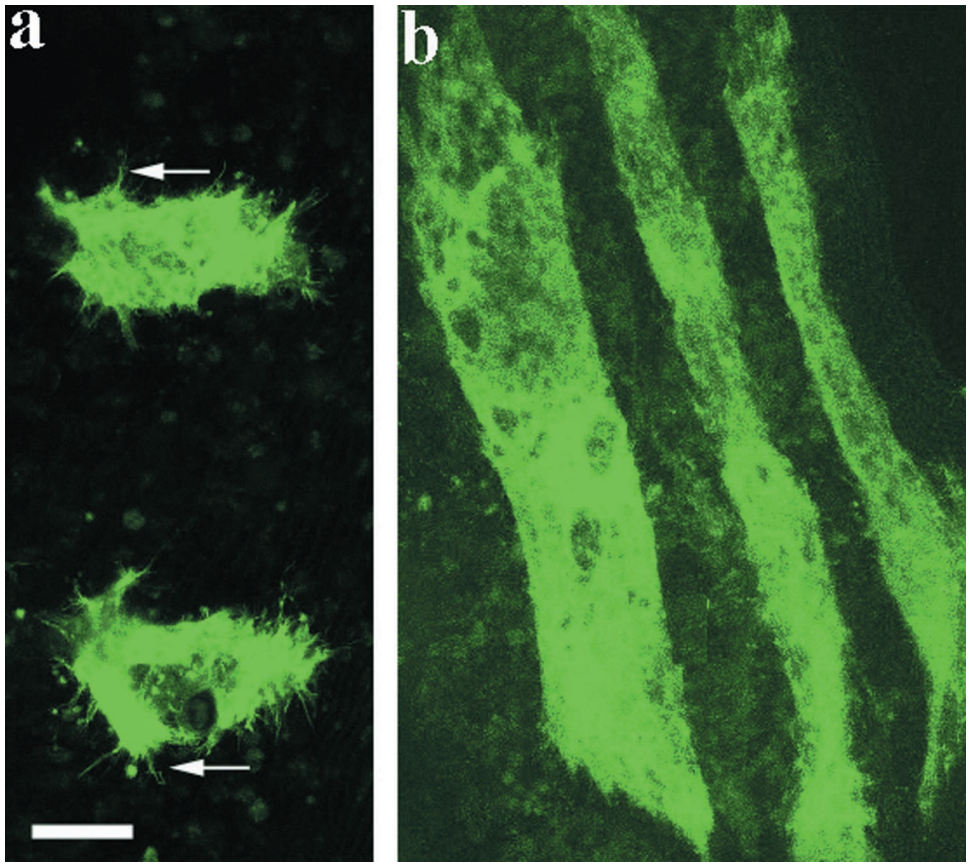

FIG. 1. GMA is an effective marker to follow morphogenetic movements in vivo. **a:** Confocal images of a 23-h APF 1151Gal4, UAS-GMA live pupa showing clusters of nerve-associated myoblasts in the dorsal abdominal hemisegments A3 and A4. GMA accentuates the shape of the myoblast clusters and reveals fine, actin-rich extensions protruding from the myoblasts (indicated by arrows). **b:** A 12-h APF *duf*-Gal4, UAS-GMA live pupa showing the three larval templates in the mesothorax. Both images were collected with a 0.8 NA, 25× multi-immersion objective on a Zeiss LSM 510 confocal microscope. Anterior is to the top and dorsal midline is to the left. A 40-μm scale bar is shown for **a** and **b** in **a**.

creases the quantum efficiency of GFP and fly codon bias is very similar to human codon bias, so the chimeric protein is expected to and does express well in fly tissues. In the chimeric GMA construct the GFP stop codon is replaced with a codon that encodes leucine (TGA to CTT). The very next codon is the naturally occurring one that encodes the leucine (CTG) that is 140 amino acids upstream of the C-terminus of *Drosophila* moesin (the protein junction is LYKLLQD, where LYK is from GFP, L is added in construction of the chimera, and LQD is from moesin). This chimeric construct was cloned directly into the pUAST vector using the EcoRI-NotI restriction sites, transgenics were generated by standard methods, and independent lines bearing insertions in all three chromosomes were obtained (Bloor and Kiehart, 2001). Insertion of the construct had no harmful effect on fly development or behavior even when expressed ubiquitously (unpublished data on UAS-GMA; see Kiehart *et al*. [2000] for ubiquitous expression of a related construct that includes the extended alpha helical region of moesin). When GMA protein was expressed in specific tissue types, by crossing the transgenics to different Gal4 drivers, both portions of the chimeric protein were found to retain their normal in vivo functions: the GFP portion yielded bright fluorescence in living cells while the moesin tail associated with actin-rich cell cytoskeleton, thereby accentuating cell shape and cell surface projections (Fig. 1). To evaluate the effect of expression of GMA on the pattern of actin in cells, we expressed the construct in a striped pattern in *Drosophila* embryos using *paired* or *engrailed* Gal4 as a driver. Specimens were then fixed and stained with rhodamine phalloidin. The distribution of actin in epithelial cells that were expressing GMA is indistinguishable from the distribution of actin in cells in adjacent stripes that are not expressing the construct (Fig. 2), demonstrating that this construct has no effect on the overall distribution of actin in living cells. All the transgenic lines produced indistinguishable results.

We next used UAS-GMA to visualize live cell movements and tissue interactions in living embryos and pupae. For our studies, we used a transgenic line bearing the insert in the third chromosome and concentrated on two developmental events: the formation of the somatic muscles in the embryo and the histolysis of larval muscles during pupal myogenesis.

In embryos, the regularly arrayed somatic muscles constitute the most well-studied derivative of mesoderm. Each somatic fiber is seeded by a special myoblast, the "founder" myoblast (Bate, 1993). Once the founders are specified at the correct position, subsequent events involving myoblast migration, aggregation, and fusion produce the syncytial fibers. The entire process spans from embryonic stage 12 to stage 15, which corresponds to ~7.20 h to 13 h AEL (after egg lay), respectively, at 25°C.

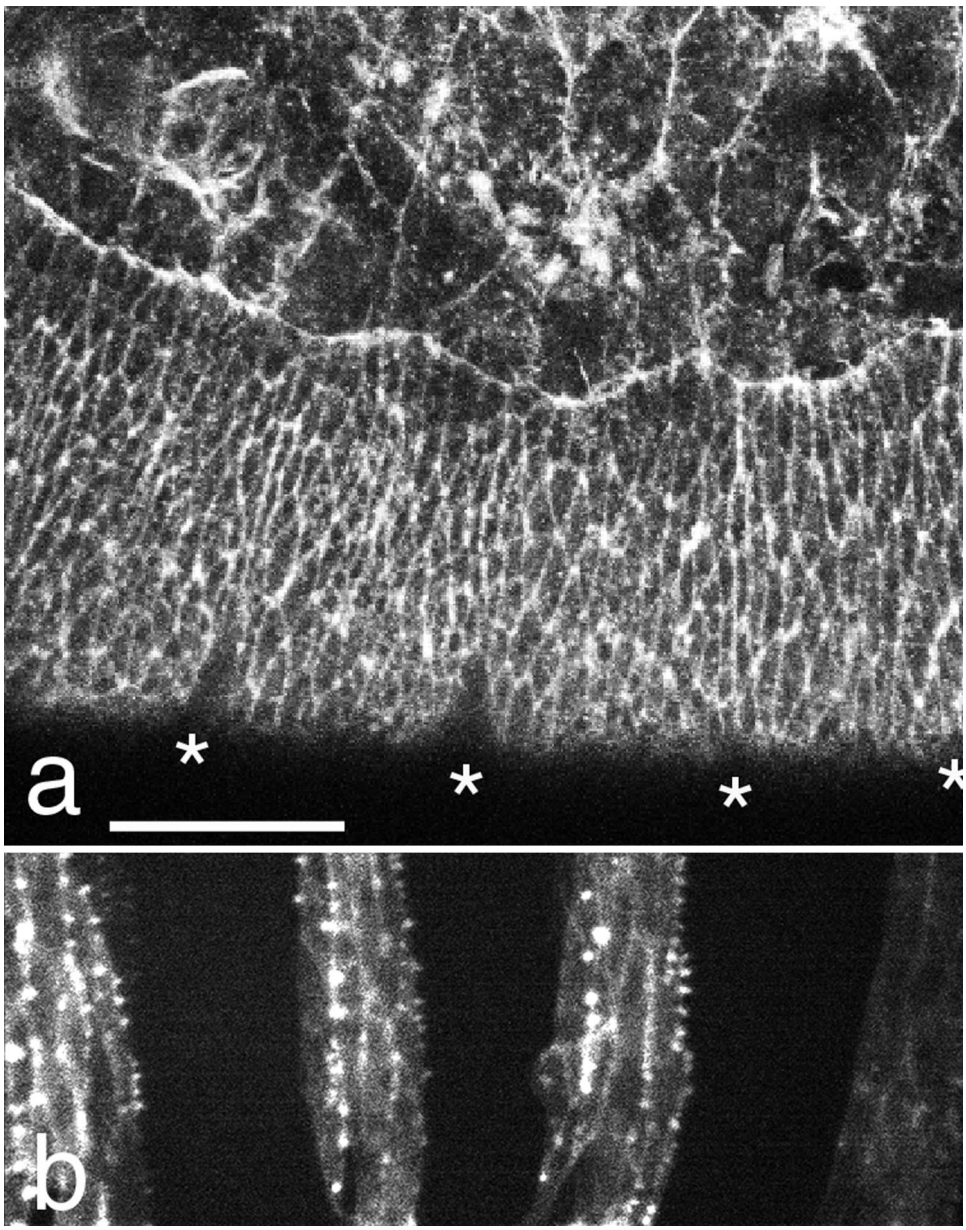

FIG. 2. Actin distribution in not affected by the expression of GMA. Confocal micrographs demonstrate that expression of GMA does not alter the distribution of actin in cells. GMA was expressed using *engrailed*-Gal4 (detailed in Bloor and Kiehart, 2002). **a:** This embryo was fixed and stained with rhodamine-phalloidin to assess the distribution of actin in GMA-expressing cells and in adjacent, nonexpressing stripes using the red fluorescent channel (under the fixation conditions we used, fluorescence due to GFP in the green channel is abolished). **b:** A different embryo at a comparable stage and magnification to establish the spatial periodicity and extent of engrailed-driven, GMA expression. The width of the engrailed expressing stripe is wider than expected due to the perdurance of both the Gal4 and GMA proteins. Asterisks in **a** indicate segmental boundaries. Note that the pattern of actin in cells in the GMA expressing stripes is indistinguishable from adjacent, non-GMA-expressing cells, indicating that GMA does not alter the cellular content or distribution of actin. Panel **a** was taken with a 1.2 NA, 63× water immersion objective on a Zeiss 510 LSM; panel **b** was taken with a 1.2 NA, 40× on a Zeiss Axioplan stand fitted with a Perkin-Elmer spinning disk confocal imaging head. The 35-μm scale bar in **a** is for **a** and **b**.

To image embryonic somatic myogenesis, we crossed UAS-GMA to *dumbfounded* (*duf*)-Gal4, a founder specific Gal4 driver (M. Ruiz-Gomez and M. Bate, pers. commun.; see also Ruiz-Gomez *et al*., 2000). *duf*-Gal4 expression is initiated in the founder cells and continues within the growing myotubes. Embryos from the above cross were aged for 7–8 h at 25°C and imaged live for 10 h using confocal microscopy at 20–22°C. Time-lapse images demonstrated the overall development of the somatic muscles. At the magnification at which we acquired the images, single founder cells were not observed. But progressively the growing myotubes appear and their transformation into fully-formed muscle fibers was recorded (Fig. 3). Particularly prominent in the images is the active movement of the growth-cone-like processes put out by muscle primordia (Fig. 4). The growing tip can be seen exploring the surface of the epidermis for its attachment site (Figs. 3d,e, 4) and subsequently forming stable attachment (Fig. 3h) .

With the onset of metamorphosis, the larval muscles begin to histolyse and their remains are phagocytosed. Concurrently, the adult myoblasts, which had remained associated with imaginal discs (in thoracic segments) or with peripheral nerves (in thorax and abdomen) during the larval life, migrate out to precise spatial locations and fuse to form the new set of adult muscles (Bate, 1993). Histolysis of muscles in the thoracic and abdominal segments occurs in two distinct phases. The first phase, occurring very early during metamorphosis, involves the degeneration of most of the thoracic muscles. One set of muscles that escape histolysis in this phase are the larval internal dorsal oblique muscles (DA1, 2,3) which are

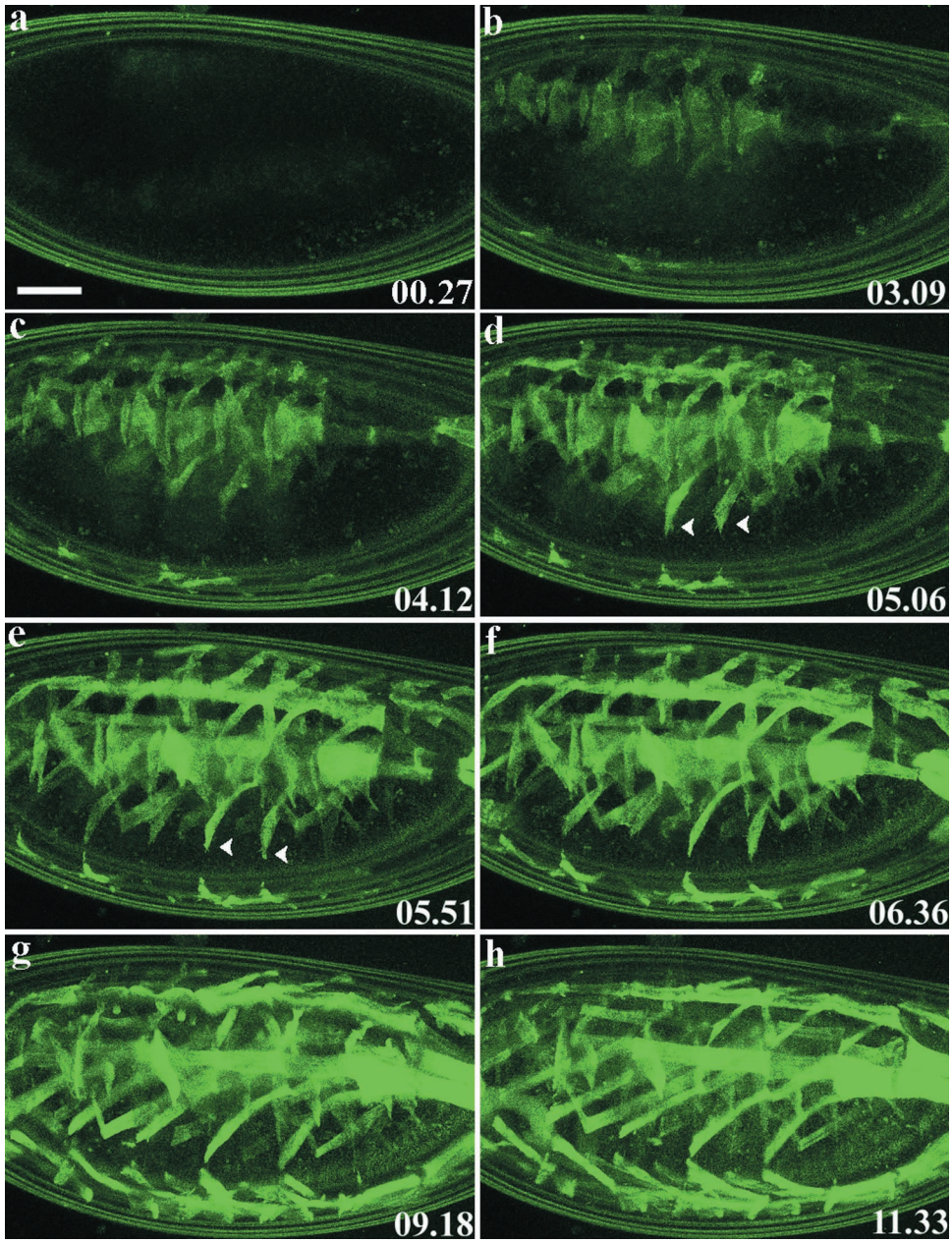

FIG. 3. Somatic myogenesis in a developing embryo. **a–h:** Selected images from a time-lapse confocal sequence of somatic muscle biogenesis in a *duf*-Gal4, UAS-GMA embryo. Time in hours: minutes is given in the lower right, with 00.00 representing the start time of imaging. **a:** The age of the embryo corresponding to this image is 8.5 h AEL. At this stage, single *duf*-expressing founder myoblasts appear in the somatic mesoderm but is not resolvable under these conditions. **b,c:** With increasing accumulation of GMA, the developing myotubes become clearly visible. **d,e,f:** Growing tips of myotubes send out filopodial extensions as they migrate toward their insertion sites on the epidermis. Extensions projecting from two syncytial myofibers are indicated by arrowheads. **h:** Fully-formed set of somatic muscles in the embryo (see also Movie 1). The flies for the *duf*-Gal4×UAS-GMA cross were cultured in small population cages. Embryos were collected in grape juice plates for 1 h in 25°C and further aged for 7 h. Next, embryos were dechorionated by gently teasing with forceps, immersed in a 1:1 mixture of halocarbon 27 and 700 (Halocarbon Products Corp., N. Augusta, SC) and mounted in an oxygen-permeable Teflon window chamber which allowed development to proceed. A single embryo was imaged once in every 9 min for a period of 10 h using a Zeiss LSM 510 confocal microscope with 25× multi-immersion 0.8NA Zeiss objective. For each timepoint a stack of Z-sections were taken which were reconstructed into a single 3D image. These series of images can be played back as QuickTime movies (Movie 1). Scale bar in **a** is 50 μm and is for all panels.

FIG. 4. Dynamic movement of filopodia in the growing myotubes. **a–f:** Series of successive time point images (corresponding to frames 46–51 of Movie 2) during embryonic myogenesis, showing the active movement of muscle filopodia. The growing myotubes are involved in the continuous process of extending and retracting filopodial extensions in search of correct attachment site. The white arrows in **a,b,c** trace one such filopodial extension which is in the process of being withdrawn. A new filopodia being sent out by an adjacent muscle fiber is indicated by arrowhead in **d,e,f.** Time in hours:minutes (from the start of the time-lapsed sequence) is given in the bottom right-hand side. A single embryo was imaged once every 9 min for a period of 10 h using a Zeiss LSM 510 confocal microscope with 25× multi-immersion 0.8NA Zeiss objective. These series of images are included in QuickTime Movie 2. Scale bar in **a** is 30 μm and is for all panels.

FIG. 5. Larval muscle degeneration viewed live in a metamorphosing pupa. **a–i:** Images from selected time points of a time-lapse imaging study of *Mhc*-GAL4, UAS-GMA pupa showing events of thoracic muscle degeneration during early metamorphosis. **a:** Intact larval muscles present in a 0-h APF pupa. The denticle belts in the pupal case (arrow) are autofluorescing. **b,c,d:** Progressive degeneration of the muscles in the thoracic segments. The small arrowhead follows the gradual histolysis of one dorsal muscle fiber. **e:** Thoracic muscle histolysis is 100% complete. Note the intact abdominal muscles (big arrowhead) whose histolysis begins at a later time period (at around 24 h APF). Surprisingly, the larval templates are not observed here. **f,g,h,i:** The larval templates start becoming visible. In (**f**) and (**i**) the templates are marked by white asterisks (see also Movie 3). The *Mhc*-GAL4 ×UAS-GMA cross was maintained in normal fly food media. 0-h APF pupae were collected, glued to the membrane of the Teflon windowed chamber with the dorsal side up, and imaged once every 8 min for 11 h with a Zeiss LSM 510 confocal microscope using a 10× dry, 0.50 NA Zeiss objective. In all images anterior is to the top and dorsal side is facing up. Scale bar in **a** is 200 μm and is for all panels.

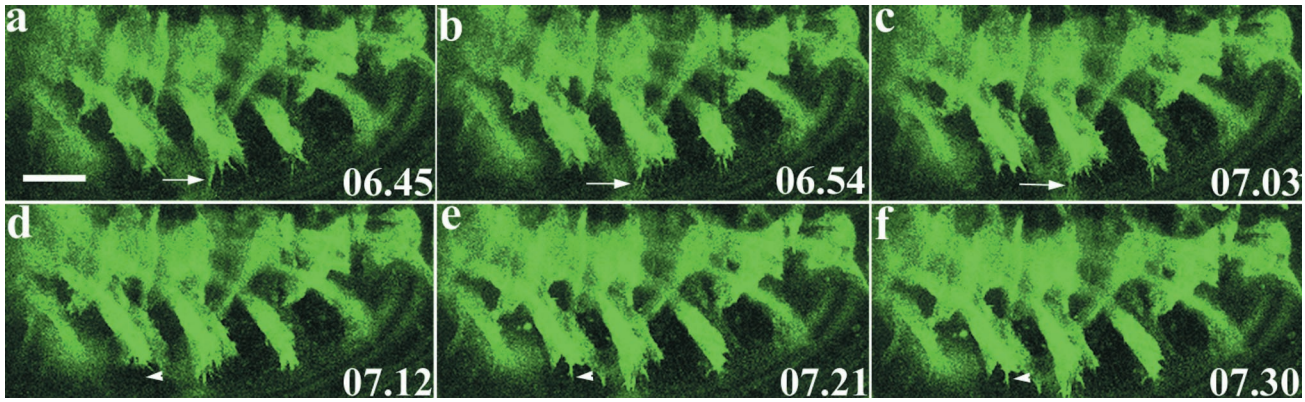
a
06.45
b
06.54
c
07.03
d
07.12
e
07.21
f
07.30

FIG. 4

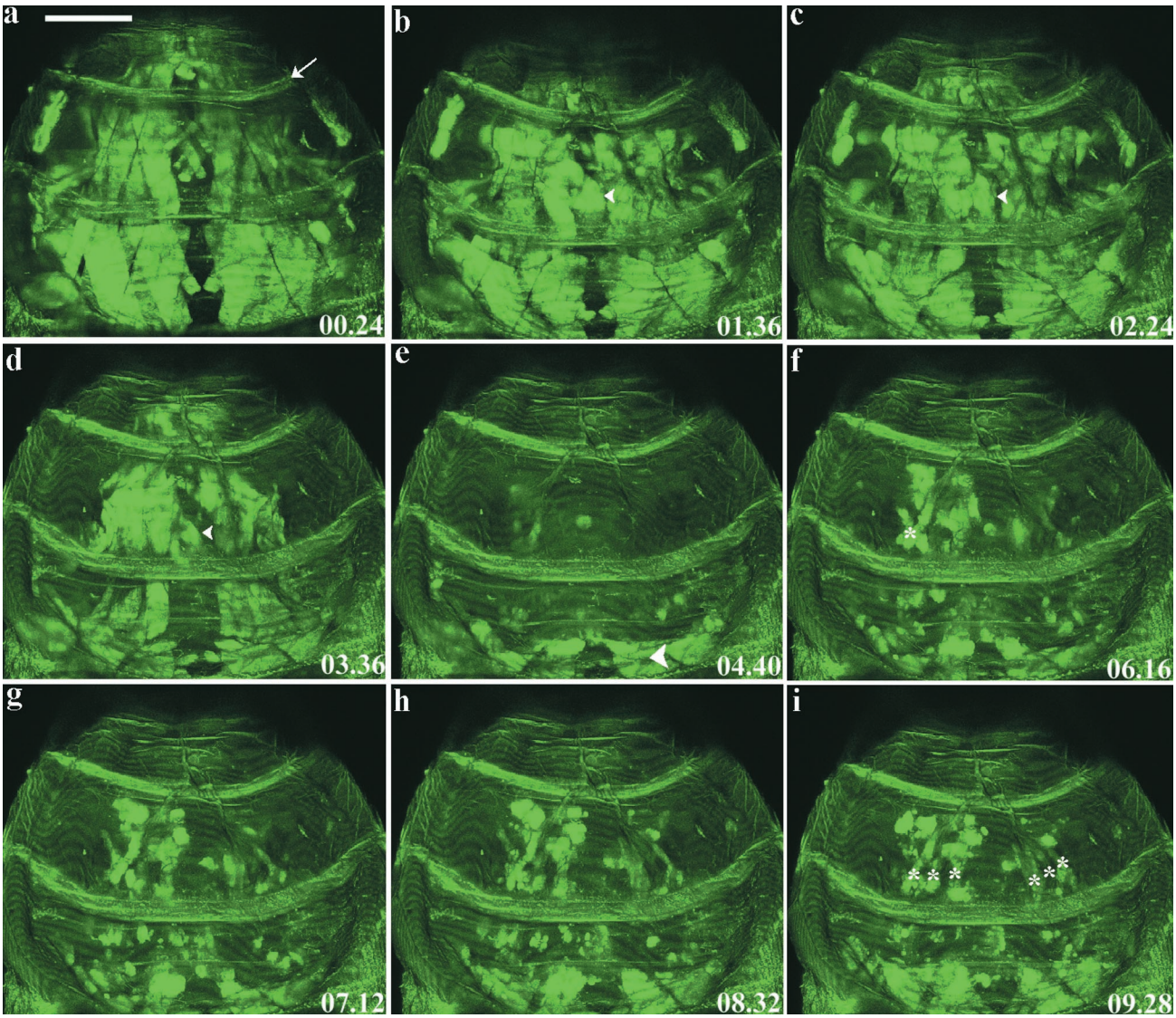
a
00.24
b
01.36
c
02.24
d
03.36
e
04.40
f
06.16
g
07.12
h
08.32
i
09.28

FIG. 5

subsequently remodeled to function as "templates" for the dorsal longitudinal muscles (DLMs) in the mesothorax (Fernandes *et al*., 1991). The abdominal muscles degenerate at a later time point, beginning around 20 h APF (after puparium formation).

Using UAS-GMA, we imaged the histolysis of thoracic muscles in the metamorphosing pupa. For labeling the muscles we used the muscle *myosin heavy chain* (*Mhc*)-Gal4 driver, a homozygous viable line on the third chromosome containing a muscle *mhc* promoter fused to the open reading frame of Gal4 (Davis *et al.,* 1997). *Mhc*-Gal4 drives expression exclusively in muscles beginning in the early first larval instar. At the beginning of metamorphosis *mhc* expression is shut off but both the Gal4 and the GMA proteins perdure. Imaging the pupa from 0 h APF to 11 h APF captured the progressive degradation of the thoracic muscles (Fig. 5). The first signs of muscle degradation appeared at around 56 min APF and by 4 h APF the histolysis of the muscles was complete. The abdominal muscles remained intact throughout the period of imaging.

Real-time imaging of thoracic muscle histolysis produced a tantalizing observation. There was a brief period, between 4.5 h APF to 5 h APF, when the DLM templates were totally absent (see Fig. 5d). The templates appeared only after 5 h APF. This observation is in apparent contradiction to our present understanding of the templates. Because of the long perdurance of both *mhc* GAL4 and the GMA actin marker, we are convinced that this is not because the markers are absent. The unhistolysed fibers undergo dramatic morphological rearrangements, including vacoulation and changes in shape, prior to their transformation into "templates" (Fernandes *et al*., 1991). There have also been suggestions of extensive cytoskeletal reorganization occurring in the very early stages in these fibers (Fernandes *et al*., 1991; Tiegs, 1955). Our data probably hint to such reorganizations and studies to explain it are being pressed presently. A point that needs to be kept in mind is that our imaging was done at ~20–22°C. At this temperature, development of the animal is slower compared to conditions normally cited in the literature (25°C). Thus, the duration and timing of various developmental events may appear to be longer and retarded compared to "standards" established by previous studies (e.g., Fernandes *et al.,* 1991). Nevertheless, these data establish a spatial–temporal reference frame which, aided with genetic and molecular data, should be helpful in understanding the orchestrated process of pupal muscle histolysis.

High fluorescence signal, high-affinity actin-binding activity, and innocuous behavior within the cell makes UAS-GMA an invaluable tool for live imaging of morphogenetic events over long hours and at high spatial resolution. Imaging of wild-type behavior can further form the basis for large-scale screening for mutants that are defective in these events. Additionally, the ability of GMA and the construction of new spectral variants (YMA, CMA, etc.) to illuminate actin cytoskeleton dynamics suggests important applications in studies concerning cell cytoskeletal architecture (Edwards *et al*., 1997; Kiehart *et al*., 2000; Bloor and Kiehart, 2001, 2002).

ACKNOWLEDGMENTS

We thank Michael Bate and Christoph Schuster for the Gal4 fly stocks. DD thanks Jayan Nair and all members of Kiehart lab for their assistance. DD is partly supported by the Kanwal Rekhi Fellowship.

LITERATURE CITED

Bate M. 1993. The mesoderm and its derivatives. In: Bate M, Martinez-Arias A, editors. The development of *Drosophila melanogaster,* vol. 2. New York: Cold Spring Harbor Laboratory Press. p 1013–1090.

Brand AH, Perrimon N. 1993. Targeted gene expression as a means of altering cell fates and generating dominant phenotypes. Development 118:401–415.

Brand AH, Manoukian AS, Perrimon N. 1994. Ectopic expression in *Drosophila*. In: Goldstein LSB, Fyrberg EA, editors. *Drosophila melanogaster*: practical uses in cell and molecular biology. San Diego: Academic Press. p 635–654.

Bloor JW, Kiehart DP. 2001. *zipper* nonmuscle myosin-II functions downstream of PS2 integrin in *Drosophila* myogenesis and is necessary for myofibril formation. Dev Biol 239:215–228.

Bloor JW, Kiehart, DP. 2002. RhoGTPase function during epithelial development. Development 129:3173-3183.

Chalfie M, Kain S. 1998. Green fluorescent protein: properties, applications and protocols. New York: John Wiley & Sons.

Davis GW, Schuster CM, Goodman CS. 1997. Genetic analysis of the mechanisms controlling target selection: target-derived Fasciclin II regulates the pattern of synapse formation. Neuron 19:561–573.

Edwards KA, Montague RA, Shepard S, Edgar BA, Erikson RL, Kiehart DP. 1994. Identification of *Drosophila* cytoskeletal proteins by induction of abnormal cell shape in fission yeast. Proc Natl Acad Sci USA 91:4589–4593.

Edwards KA, Demsky M, Montague RA, Weymouth N, Kiehart DP. 1997. GFP-moesin illuminates actin cytoskeleton dynamics in living tissue and demonstrates cell shape changes during morphogenesis in *Drosophila.* Dev Biol 191:103–117.

Fernandes J, Bate M, Vijayraghavan K. 1991. Development of the indirect flight muscles of *Drosophila*. Development 113:67–77.

Furthmayr H, Lankes W, Amieva M. 1992. Moesin, a new cytoskeletal protein and constituent of filopodia: its role in cellular functions. Kidney Int 41:665–670.

Hazelrigg T. 1998. The uses of green fluorescent protein in *Drosophila.* In: Chalfie M, Kain S, editors. Green fluorescent protein: properties, applications and protocols. New York: John Wiley & Sons. p 169–190.

Kiehart DP, Galbraith C, Edwards KA, Rickoll WL, Montague RA. 2000. Multiple forces contribute to cell sheet morphogenesis for dorsal closure in *Drosophila*. J Cell Biol 149:471–490.

Nakamura F, Huang L, Pestonjamasp K, Luna EJ, Furthmayr H. 1999. Regulation of F-actin binding to platelet moesin in vitro by both phosphorylation of threonine 558 and polyphosphatidylinositides. Mol Biol Cell 10:2669–2685.

Pollard TD, Blanchoin L, Mullins RD. 2000. Molecular mechanisms controlling actin filament dynamics in nonmuscle cells. Annu Rev Biophys Biomol Struct 29:545–576.

Ruiz-Gomez M, Coutts N, Price A, Taylor MV, Bate M. 2000. *Drosophila* dumbfounded: a myoblast attractant essential for fusion. Cell 102: 189–198.

Tiegs OW. 1955. The flight muscles of insects. Philos Trans R Soc Lond B 238:221–348

Tsien R, Prasher D. 1998. Molecular biology and mutation of green fluorescent protein. In: Chalfie M, Kain S, editors. GFP: green fluorescent protein. Properties, applications, and protocols. New York: John Wiley & Sons. p 97–118.

van Roessel P, Brand AH. 2002. Imaging into the future: visualizing gene expression and protein interactions with fluorescent proteins. Nat Cell Biol 4:E15–E19.

Verkhusha VV, Tsukita S, Oda H. 1999. Actin dynamics in lamellipodia of migrating border cells in the Drosophila ovary revealed by a GFP-actin fusion protein. FEBS Lett 445:395–401.